ARTICLES

Experimental and Theoretical Studies of the Reactions of Excited Calcium Atoms with Ethyl and *n*-Propyl Bromides

Ke-Li Han,* Li Zhang, Da-Li Xu, Guo-Zhong He, and Nan-Quan Lou

State Key Laboratory of Molecular Reaction Dynamics, Dalian Institute of Chemical Physics, Chinese Academy of Sciences, Dalian 116023, China

Received: June 16, 2000; In Final Form: January 18, 2001

To study the effect of the orbital alignment of $Ca(^1P_1)$ on the product alignment, we have probed the CaBr-$(B^2\Sigma^+)$ product rotational alignments in the reactions of $Ca(^1P_1)$ with C_2H_5Br and *n*-C_3H_7Br by means of laser-induced chemiluminescence under single-collision conditions in a beam-gas arrangement. When the laser polarization vector is parallel to the Ca beam for the reaction $Ca(^1P_1) + C_2H_5Br$, the rotation of the $CaBr(B^2\Sigma^+)$ product seems to be more strongly aligned in comparison with that when the laser polarization vector is perpendicular to the Ca beam but when there is significant overlapping of error bars. However, for the reaction $Ca(^1P_1) + n$-C_3H_7Br, there is no statistical difference in the product rotational alignment when the $Ca(^1P_1)$ atomic orbital alignment is changed. The values of $\langle P_2(\hat{\mathbf{J}}'\cdot\hat{\mathbf{k}})\rangle$ become less negative as the number of carbons is increased, which is probably attributed to the differences in the mass factors and potential energy surfaces. Quasiclassical trajectory (QCT) based on a LEPS potential energy surface (PES) has been employed to interpret the experimental results.

1. Introduction

The effect of reagent approach geometry on chemical reactions is an interesting field of dynamical stereochemistry. However, the direct interrogation of reactive geometric requirements is difficult, and only a few such studies have been carried out. External fields have been employed to prepare oriented or aligned polar symmetric top molecules.[1−4] Recently, polarized lasers have been extensively used to prepare aligned excited molecules.[5−9] An important new class of experiments aimed at steric control of reagents takes advantage of orbital alignment or orientation of atomic reagents achieved by polarized laser excitation. An example of an inelastic atom−molecule collision involving orbital alignment is the study of[10]

$$Na(3p) + H_2(v=0) \rightarrow Na(3s) + H_2(v=1,2,3) \qquad (1)$$

The alignment of the Na p orbital with respect to the relative velocity vector is found to influence the outcome of the collision. Somewhat more relevant to the chemical domain is the extension of this technique to reactive encounters by Zare and co-workers,[11] as exemplified by the reaction

$$Ca(^1P_1) + HCl \rightarrow CaCl(B^2\Sigma^+, A^2\Pi) + H \qquad (2)$$

Here the perpendicular (π) alignment of the Ca p orbital, which favors $CaCl(A^2\Pi)$ formation, is less effective in forming the $B^2\Sigma^+$ product; the parallel (σ) alignment favors the formation of the $B^2\Sigma^+$ state and is less effective in producing the $A^2\Pi$ state. Recently, Lee and co-workers[12] have conducted crossed-beam studies of reactions of aligned excited alkali atoms with hydrogen chloride, oxygen, and nitrogen dioxide. With the alkali valence electron in the 3p, 4d, or 5s orbital, the product angular and velocity distributions varied markedly with the collision energy, the symmetry of the atomic state, and the alignment of the excited 3p or 4d orbitals. Most recently, Ding et al.[13] showed that orbital alignment of $Ca(^1P_1)$ colliding with CH_3I can influence the CaI product vibrational distributions.

It is very important that the product rotational alignment is determined since the rotational angular momentum vector is preferentially oriented and aligned with respect to the colliding reagents. For excited-state products, spatial product anisotropy can be probed by the polarization-resolved chemiluminescent method. For ground-state products, polarized laser-induced fluorescence and electric deflections of the product can be employed to measure the spatial distribution of product vector properties about an experimentally defined initial axis of symmetry. Linearly polarized lasers have been widely used to detect product rotational alignment, whereas circularly polarized laser beams have been used to measure the product rotational orientation.[14] Moreover, the use of polarized lasers for both initiation and probing stages of a photon-initiated reaction sequence can in principle provide a means of probing product-state-resolved rotational polarization as a function of center-of-mass (CM) scattering angle.[9,15] Indeed, the effect on product rotational alignments, including state-selective ones of the reactants' vibrational, rotational, and translational energies for a large number of systems, has been studied in detail recently.

A problem of considerable interest in stereodynamics is how the potential energy surface (PES) affects the product rotational alignment, i.e., the distribution of the product angular momentum vectors. As pointed out in a previous paper,[16] for several

* Corresponding author. E-mail: klhan@dicp.ac.cn.

10.1021/jp002181x CCC: $20.00
Published on Web 03/14/2001

different mass combinations except of H + HL (H, heavy; L, light) on a simple PES with the reaction barrier located in the entrance valley, the product rotation will be strongly aligned. On the other hand, if the reaction barrier is located in the exit valley, the product rotation will be less aligned. But for H + HL reactions, the product rotational alignment is independent of the reaction barrier location since the kinematic limit for this class of reactions is the complete disposal of the initial orbital (**L**) into the product rotational (**J′**) angular momentum. However, in a real chemical system, the PES is seldom known, and sometimes several PESs are involved along the reactive path. The direct experimental measurement of the product rotational alignment, particularly the translational energy dependence of the product rotational alignment, together with excitation function and the product internal distributions, can provide the fullest probe of these potential surfaces.

The measurement of the product rotational alignment has special interest in those reactions having the mass combination

$$H + H'L \rightarrow HH' + L \tag{3}$$

although very little information on the potential energy surfaces can be obtained from those reactions.[16] As is well-known for these kinematically constrained reactions, as the mass factor

$$\cos^2 \beta = \frac{m_H m_L}{(m_H + m_H)(m_H + m_L)} \tag{4}$$

approaches zero, the product rotational angular momentum vector is strongly aligned with respect to the relative velocity direction. The product rotational alignment, however, strongly depends on the mass factor $\cos^2 \beta$ of the reactive system.[14,16] The increase in mass factor $\cos^2 \beta$ will reduce the anisotropic distribution of **J′** by about **k** but enhance the probability of probing potential surfaces.[16] With respect to this kind of problem, the reactions of alkaline earth metals with halogenated molecules have been extensively studied.[22−32]

In this paper, we report the investigation of the effect of the alignment of laser-excited $Ca(^1P_1)$ on the rotational alignment of the $CaBr(B^2\Sigma^+)$ products from chemiluminescent reactions

$$Ca(^1P_1) + C_2H_5Br \rightarrow CaBr(A^2\Pi; B^2\Sigma^+) + C_2H_5 \tag{5}$$

$$Ca(^1P_1) + n\text{-}C_3H_7Br \rightarrow CaBr(A^2\Pi; B^2\Sigma^+) + n\text{-}C_3H_7 \tag{6}$$

2. Experiment

The experimental apparatus was essentially the same as that previously reported,[14,17−19] although the setup was slightly rearranged for the laser-induced chemiluminescent experiment. Metallic Ca is heated to 1030 K in an oven. The beam of metal atoms effuses from the oven and then enters the reaction chamber through a 0.3×1 cm^2 rectangular hole. The reaction chamber has been filled with the reactant gas. The pressure of the reactant gas is lower than 0.02 Pa to satisfy single collision conditions. The 99% pure C_2H_5Br and *n*-C_3H_7Br samples were commercially purchased from Beijing Chemical Company.

Orbitally aligned $Ca(^1P_1)$ atoms are readily obtained by the absorption of polarized light at 422.7 nm from a dye laser pumped by an Ar^+ laser (model 2045E). A laser-power gauge behind the window of the reaction chamber monitors the laser power to make sure that the laser power does not change during the experiment, especially when the laser polarization vector **E** is rotated. In the excitation zone, the laser power is approximately 180 mW and ≥90% polarized. The polarization vector of linearly polarized laser light is rotated by a Fresnel rhomb.

The chemiluminescence of the nascent product CaBr(B) is collected by a 15 cm focal length lens positioned at right angles to both the atomic beam and the laser beam. A film polarizer is placed in front of a 1 m monochromator. A photomultiplier (RCL C31034) is placed behind the monochromator to detect both perpendicular and parallel components of the chemiluminescence. The output of the PMT is measured by a lock-in amplifier. The response of the optical system, including the monochromator, to the polarized light has been carefully calibrated.

An additional photomultiplier (PMT 2, 9558QB) is placed at a 45° angle to the laser beam and at a 90° angle to the metal beam axis to monitor the $Ca(^1S_0-^1P_1)$ fluorescence. All signals fall to the baseline when either the reagent gas or the laser is blocked. For the highest powerful sensitivity of the light-detection system, the atomic $Ca(^1S_0-^1D_2)$ and $Ca(^1S_0-^3P_1)$ lines were not detected. These results indicate that $Ca(^3P_1)$ and $Ca(^1D_2)$ make a negligible contribution to the processes studied here.

3. Results and Discussion

A. Rotational Alignment of CaBr($^2\Sigma^+$). During reactive encounters, the total angular momentum is conserved

$$\mathbf{J} + \mathbf{L} = \mathbf{J}' + \mathbf{L}' \tag{7}$$

where **L** and **L′** are the orbital momenta of reactant and product, respectively. When the reactant angular momentum **J** is small (as is common), the product rotational angular momentum can only result from **L**. The distribution of the angular momentum **J′** of the product molecule is described by a function $f(\hat{\mathbf{J}}'\cdot\hat{\mathbf{Z}})$. The usual experimental configurations possess cylindrical symmetry in space, and a cylindrically symmetric distribution of rotational angular momentum of products can be expressed as a Legendre expansion

$$f(\hat{\mathbf{J}}'\cdot\hat{\mathbf{Z}}) = \sum_l a_l P_l(\hat{\mathbf{J}}'\cdot\hat{\mathbf{Z}}) \tag{8}$$

in which the $\hat{\mathbf{Z}}$ denotes the symmetry axis and superscript carats denote unit vectors. The expression

$$\hat{\mathbf{J}}'\cdot\hat{\mathbf{Z}} = \cos\theta \tag{9}$$

is the cosine of the angle between $\hat{\mathbf{J}}'$ and $\hat{\mathbf{Z}}$, and the coefficients

$$a_l = \frac{2l+1}{2}\int_{-1}^{1} P_l(\hat{\mathbf{J}}'\cdot\hat{\mathbf{Z}})f(\hat{\mathbf{J}}'\cdot\hat{\mathbf{Z}})d(\hat{\mathbf{J}}'\cdot\hat{\mathbf{Z}})$$
$$= \frac{2l+1}{2}\int_{-1}^{1}\langle P_l(\hat{\mathbf{J}}'\cdot\hat{\mathbf{Z}})\rangle \tag{10}$$

are the *l*th Legendre moments of the distribution $f(\hat{\mathbf{J}}'\cdot\hat{\mathbf{Z}})$. The coefficients a_1 and a_2, which are proportional to $\langle P_1(\hat{\mathbf{J}}'\cdot\hat{\mathbf{Z}})\rangle$ and $\langle P_2(\hat{\mathbf{J}}'\cdot\hat{\mathbf{Z}})\rangle$, are used to describe the orientation and alignment of the products, respectively. (The angular brackets denote averages.)

In a chemiluminescent reaction experiment, the degree of polarization of chemiluminescence *P* can be related to the

TABLE 1: Experimental and Theoretical Results of the Rotational Alignment of CaBr($B^2\Sigma^+$)

systems	direction of laser vector **E**	degree of CL polarization	$\langle P_2(\hat{\mathbf{J}}'\cdot\hat{\mathbf{k}})\rangle$ experimental	$\langle P_2(\hat{\mathbf{J}}'\cdot\hat{\mathbf{k}})\rangle$ theoretical	mass factor $\cos\beta$
$Ca(^1P_1) + C_2H_5Br$	$\mathbf{E}\|\|\mathbf{V}_{rel}$	0.117 ± 0.015	-0.18 ± 0.02	-0.17	0.09
	$\mathbf{E}\perp\mathbf{V}_{rel}$	0.096 ± 0.015	-0.15 ± 0.02		
$Ca(^1P_1) + n\text{-}C_3H_7Br$	$\mathbf{E}\|\|\mathbf{V}_{rel}$	0.094 ± 0.015	-0.14 ± 0.02	-0.15	0.12
	$\mathbf{E}\perp\mathbf{V}_{rel}$	0.087 ± 0.015	-0.13 ± 0.02		

distribution of angular momentum vectors of the emitting molecule

$$P(P,R \text{ lines}) = \frac{-3\langle P_2(\hat{\mathbf{J}}'\cdot\hat{\mathbf{Z}})\rangle}{4 - \langle P_2(\hat{\mathbf{J}}'\cdot\hat{\mathbf{Z}})\rangle} \tag{11}$$

$$P(Q \text{ line}) = \frac{3\langle P_2(\hat{\mathbf{J}}'\cdot\hat{\mathbf{Z}})\rangle}{2 + \langle P_2(\hat{\mathbf{J}}'\cdot\hat{\mathbf{Z}})\rangle} \tag{12}$$

where $I_\perp$ and $I_{||}$ denote the CL intensities polarized parallel and

$$P = \frac{I_{||} - I_\perp}{I_{||} + I_\perp} \tag{13}$$

perpendicular, respectively, to the beam axis.

The rotational alignment in the laboratory frame is converted into the center of mass frame by using the expression

$$\langle P_2(\hat{\mathbf{J}}'\cdot\hat{\mathbf{k}})\rangle = \frac{\langle P_2(\hat{\mathbf{J}}'\cdot\hat{\mathbf{Z}})\rangle}{\langle P_2(\hat{\mathbf{k}}\cdot\hat{\mathbf{Z}})\rangle} \tag{14}$$

Under beam-gas reaction conditions, $\langle P_2(\hat{\mathbf{k}}\cdot\hat{\mathbf{Z}})\rangle$ is given by a Monte Carlo calculation.[20]

The expected values for $\langle P_2(\hat{\mathbf{J}}'\cdot\hat{\mathbf{Z}})\rangle$ are between 0.0 (randomly aligned) and -0.5 (completely aligned). Usually, when the conditions $|\mathbf{L}| \gg |\mathbf{J}|$ and $|\mathbf{L}'| \ll |\mathbf{J}'|$ are satisfied, the maximum product rotational alignment occurs. The first condition is satisfied for reactions with large cross sections, while the typical H + HL mass configuration reaction system leads to the second condition. Several example reactions are Cs + HI,HBr ($\langle P_2(\hat{\mathbf{J}}'\cdot\hat{\mathbf{k}})\rangle = -0.44, -0.38$), K + HBr ($\langle P_2(\hat{\mathbf{J}}'\cdot\hat{\mathbf{k}})\rangle = -0.42$),[21] and $Ca(^1D)$ + HCl ($\langle P_2(\hat{\mathbf{J}}'\cdot\hat{\mathbf{k}})\rangle = -0.44$).[20] For the reactions $Ca(^1P_1) + C_2H_5Br,C_3H_7Br$, the H + HL mass combination is no longer strictly appropriate. This may lead to significant $\langle P_2(\hat{\mathbf{J}}'\cdot\hat{\mathbf{k}})\rangle$ deviations from -0.5.

The chemiluminescence for the reactions studied here is detected in the range of 590−650 nm. The chemiluminescent spectra for the reactions 5 and 6 when the laser polarization vector **E** is parallel to the relative velocity are shown in Figure 1 at a resolution of 0.5 nm. The spectra are attributed to CaBr $\Delta v = 0,1$ vibrational bands of the $A^2\Pi - X^2\Sigma^+$ transition and $\Delta v = 0,1$ vibrational bands of the $B^2\Sigma^+ - X^2\Sigma^+$ transition. The experimental $\langle P_2(\hat{\mathbf{J}}'\cdot\hat{\mathbf{k}})\rangle$ values obtained from the chemiluminescent polarization P are shown in Table 1. It seems that there is very small effect of the orbital alignment of $Ca(^1P_1)$ on the rotational alignments of the CaBr($B^2\Sigma^+$) products.

The atomic p orbital charge cloud is parallel to the reagents' relative velocity vector when the laser polarization vector is parallel to the Ca beam. Here one finds that the rotation of the CaBr($B^2\Sigma^+$) product is probably more strongly aligned than when the laser polarization vector is perpendicular to the Ca beam but when there is significant overlapping of error bars. Moreover, in this case, according to refs 22 and 23, the excited product CaBr($B^2\Sigma^+$) is preferred when $Ca(^1P_1)$ approaches the Br end of the reagent molecules along the Br−C bond. The atomic p orbital charge cloud is perpendicular to the Ca beam when the laser polarization vector is perpendicular to the Ca beam. In this case, it seems that the rotation of the CaBr($B^2\Sigma^+$) product is less aligned. The reaction preferentially produces the excited CaBr($A^2\Pi$) product. The effect of the orbitally aligned $Ca(^1P_1)$ on the product alignment for the reaction $Ca(^1P_1) + C_2H_5Br$ is more significant than that for the reaction $Ca(^1P_1) + C_3H_7Br$. This may be caused by the difference in potential energy surfaces and mass factors since the product rotational alignment is sensitive to the potential energy surfaces and mass factors of reaction systems.[16,24,25]

It has been shown that the product rotational alignment is stronger for $Ca(^1P_1) + C_2H_5Br$ than for $Ca(^1P_1) + C_3H_7Br$, irrespective of alignment of the atomic orbital. This may be attributed to the mass effect; i.e., the C_3H_7 radical is heavier than the C_2H_5. The mass effect has been extensively documented for many other reactions. For the reactions $Ca(^1P_1) + CH_3I,C_2H_5I$,[22] the rotational alignment parameters of the product CaI($B^2\Sigma^+$) are -0.20 and -0.13. For $Sr(^1S_0) + CH_3Br,C_2H_5Br,C_3H_7Br$, $\langle P_2(\hat{\mathbf{J}}'\cdot\hat{\mathbf{k}})\rangle$ values are -0.34, -0.24, and -0.14, respectively.[14] For the reactions $Sr(^3P_J) + CH_3I,C_2H_5I$, the mass effect is even more significant; i.e., $\langle P_2(\hat{\mathbf{J}}'\cdot\hat{\mathbf{k}})\rangle$ values are -0.48 and -0.20, respectively.[26] This effect can be examined by performing trajectory calculations.

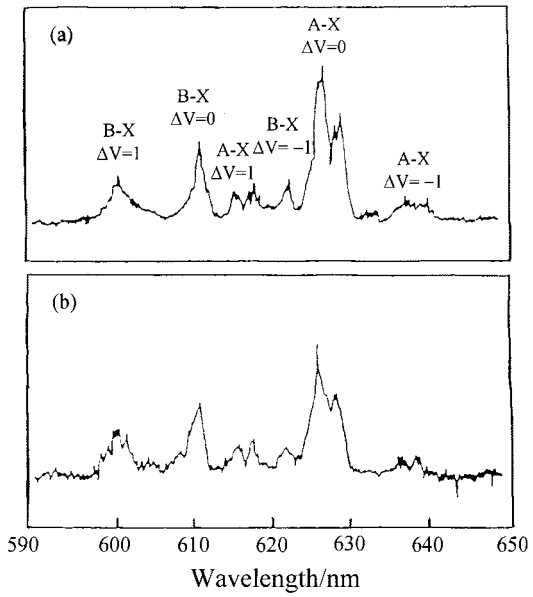

Figure 1. Chemiluminescent spectra of (a) $Ca(^1P_1) + C_2H_5Br$ and (b) $Ca(^1P_1) + C_3H_7Br$ with laser **E** vector and the emitted light parallel to the average relative velocity vector.

TABLE 2: Parameters of Potential Energy Surface for $Ca(^1P_1) + C_2H_5Br,n\text{-}C_3H_7Br$

species	D_e (eV)	β (Å^{-1})	R^0 (Å)	Sato parameter
C_2H_5Br	3.073[a]	1.681[b]	1.94	0.992
$n\text{-}C_3H_7Br$	3.024[a]	1.695[b]	1.94	0.992
CaBr[c]	4.077	0.99	2.57	0.605
RCa[d]	1.95	1.326	2.33	−0.882

[a] From ref 33. [b] From ref 35. [c] Morse parameters β and R^0 calculated from the molecular constants in ref 34. [d] Morse parameters estimated from those of $CaCH_3$.[35]

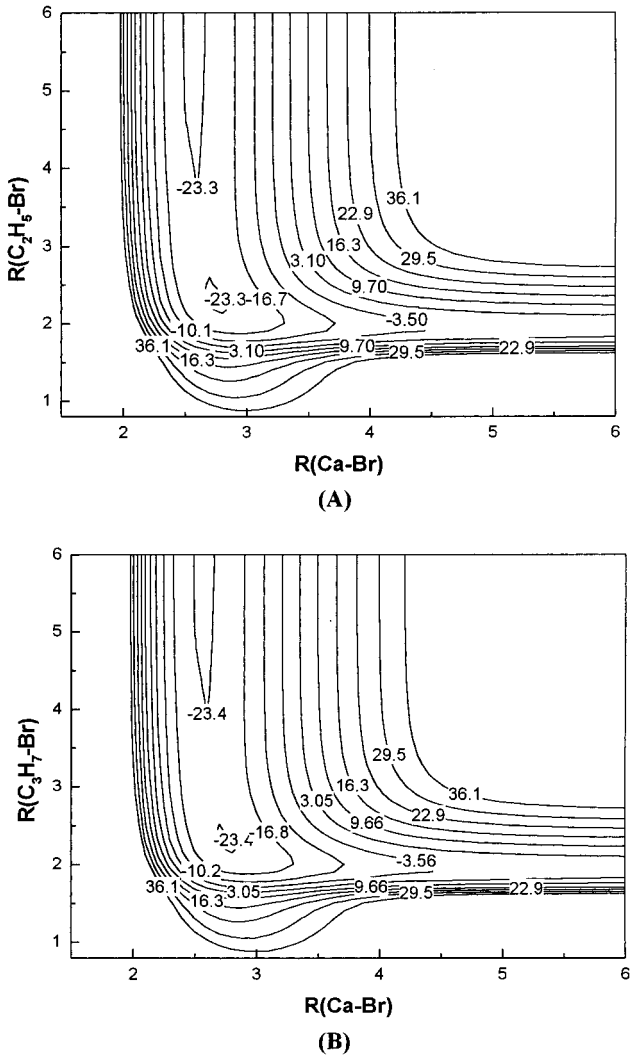

Figure 2. Potential contour map representing the model PES for the collinear configuration of the reaction Ca + C_2H_5Br (A) and the reaction Ca + C_3H_7Br (B). The contour energies are in kcal/mol, and the distances are in Å.

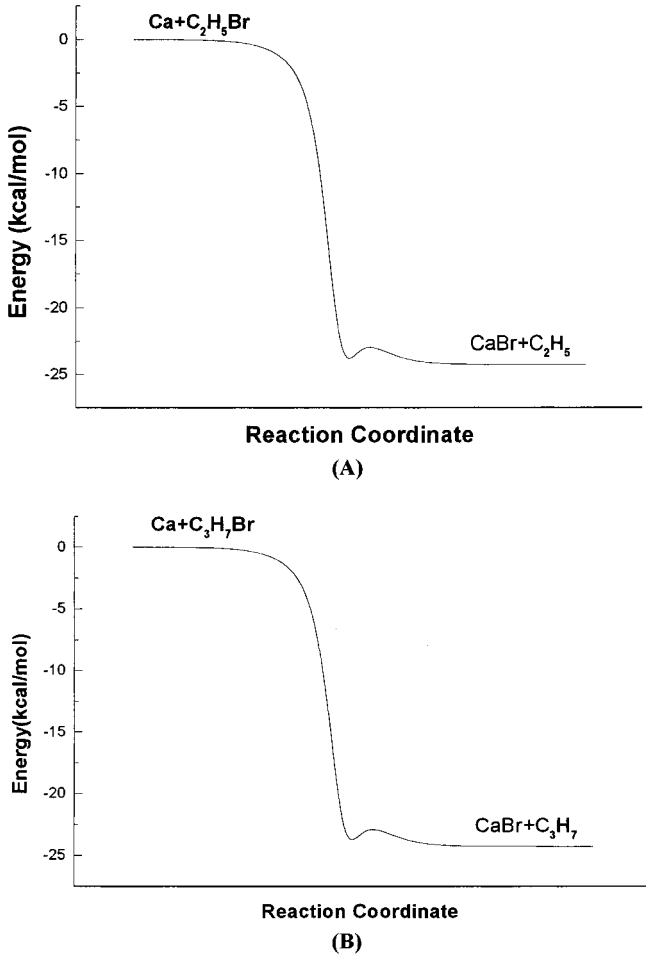

Figure 3. Reaction profile along the minimum-energy path from the reactants to products on our chosen PES of the collinear Ca + C_2H_5Br reaction (A) and the collinear Ca + C_3H_7Br reaction (B). The schematic drawing is plotted according to the LEPS potential energy surfaces that were used in QCT calculations.

B. Quasiclassical Trajectory Calculations. Extended LEPS potential energy surfaces[35,36] for the Ca($^1P_1$) + C_2H_5Br,*n*-C_3H_7-Br → CaBr(B) + C_2H_5,*n*-C_3H_7 reactions are constructed using the parameters listed in Table 2. The contour plots of these LEPS potential energy surfaces are represented in Figure 2. According to the LEPS potential energy surfaces shown in Figure 2, we also plot the reaction profiles along the minimum-energy path from the reactants to the products of the collinear Ca($^1P_1$) + C_2H_5Br,*n*-C_3H_7Br reaction which are given in Figure 3. Along the minimum-energy reaction path, there is a small potential well for both of the reactions. Trajectory calculations were performed using the well-known CLASTR program.[36] Ten thousand trajectories were sampled at the collision energy of 1.8 kcal/mol, which is the average collision energy in the experiments.

We present the QCT calculated results in Table 1. Calculated results of $\langle P_2(\hat{\mathbf{J}}'\cdot\hat{\mathbf{k}})\rangle = -0.17$ for the Ca($^1P_1$) + C_2H_5Br reaction and $\langle P_2(\hat{\mathbf{J}}'\cdot\hat{\mathbf{k}})\rangle = -0.15$ for the Ca($^1P_1$) + *n*-C_3H_7Br reaction are obtained. It is seen that, for the reaction Ca($^1P_1$) + RBr (R═C_2H_5, *n*-C_3H_7), the values of $\langle P_2(\hat{\mathbf{J}}'\cdot\hat{\mathbf{k}})\rangle$ become less negative as the number of carbons is increased, and the product rotational angular momenta $\mathbf{J}'$ tend toward a less anisotropic distribution with respect to the direction of the vector $\mathbf{V}_{rel}$. We attribute the difference in product rotational alignments $\langle P_2(\hat{\mathbf{J}}'\cdot\hat{\mathbf{k}})\rangle$ for the two reactions to both the potential energy surfaces and the mass factors. The potential energy surface of Ca($^1P_1$) + RBr has a shallow well that may affect the rotational alignment of the products. This may lead to "loss of" memory of angular momentum alignment in that the separation of the products will take various directions in space and the orbital angular momentum will also take various directions. Also, the mass combination of the Ca ($^1P_1$) + RBr reaction deviates from the H + HL mass combination. All these may lead to $\langle P_2(\hat{\mathbf{J}}'\cdot\hat{\mathbf{k}})\rangle$ distributions that deviate greatly from −0.5. Whatever the reason, the trajectory results are in very good agreement with the experimental results.

The increase of $\langle P_2(\hat{\mathbf{J}}'\cdot\hat{\mathbf{k}})\rangle$ with an increase of the length of carbon chain may be caused by differences in the mass factors and in the potential energy surfaces. However, the small differences between the contour plots of potential energy surface for the two reactions indicate that the variation of $\langle P_2(\hat{\mathbf{J}}'\cdot\hat{\mathbf{k}})\rangle$ with R group changes in R−Br molecules is probably due to the difference of the mass factor.

4. Conclusions

Experimental investigations of the product rotational alignment for the beam-gas chemiluminescence reactions Ca($^1P_1$) + R−Br(R═C_2H_5,*n*-C_3H_7) → CaBr($B^2\Sigma^+$) + R were carried out. When the excitation laser polarization vector is parallel to the Ca beam, the rotation of the CaBr($B^2\Sigma^+$) product for the reaction

$Ca(^1P_1) + BrC_2H_5$ is more strongly aligned than when the laser polarization vector is perpendicular to the Ca beam. But for the reaction $Ca(^1P_1) + n\text{-}BrC_3H_7$, there is no statistical difference in the product rotation alignment as the atomic orbital alignment is changed. The values of $\langle P_2(\hat{\mathbf{J}}'\cdot\hat{\mathbf{k}})\rangle$ become less negative as the number of carbons is increased, which is probably attributed to the differences in the mass factors and potential energy surfaces. Quasiclassical trajectories (QCT) based on LEPS potential energy surface (PES) has been employed to interpret the experimental results. The calculated results for the rotational alignment of the product are consistent with the experimental ones.

Acknowledgment. This work is supported by NKBRSF and NSFC (Grant No. 29953001). We'd like to thank the referees for their good suggestions.

References and Notes

(1) Toennies, J. P. Molecular Beam Scattering Experiments on Elastic, Inelastic and reactive Collisions. In *Physical Chemistry*; Jost, W., Ed.; Academic Press: New York, 1974; Vol. IVA, 227.

(2) Reuss, J. *Adv. Chem. Phys.* **1975**, *30*, 389.

(3) Brooks, P. R. *Science* **1976**, *193*, 11.

(4) Stolte, S. In *Atomic and Molecular Beam Methods Volume 1*; Scoles, G., Ed.; Oxford University Press: New York, 1988.

(5) Bergmann, K. In *Atomic and Molecular Beam Methods Volume 1*; Scoles, G., Ed.; Oxford University Press: New York, 1988.

(6) Zare, R. N. *Ber. Bunsen-Ges.* Phys. Chem. **1982**, *86*, 422.

(7) Han, K.-L. *Phys. Rev. A* **1997**, *56*, 4992.

(8) Zhan, J.-P.; Deng, W.-Q.; Han, K.-L.; Yang, H.-P.; He, G.-Z.; Lou, N.-Q. *Chem. Phys. Lett.* **1996**, *260*, 191.

(9) Shafer-Ray, N. E.; Orr-Ewing, A. J.; Zare, R. N. *J. Phys. Chem.* **1995**, *99*, 7591.

(10) Reitland, W.; Tittes, H. U.; Hertel, I. V. *Phys. Rev. Lett.* **1982**, *46*, 1389.

(11) Rettner, C. T.; Zare, R. N. *J. Chem. Phys.* **1987**, *77*, 2416.

(12) Vernon, M. F.; Schmidt, H.; Weiss, P. S.; Covinsky, M. H.; Lee, Y. T. *J. Chem. Phys.* **1986**, *84*, 5580.

(13) Ding, G.; Sun, W.; Yang, W.; Xu, D.; He, G.; Lou, N. *Chem. Phys. Lett.* **1997**, *265*, 392.

(14) Li, R.-J.; Han, K.-L.; Li, F.-L.; Lu, R.-C.; He, G.-Z.; Lou, N.-Q. *Chem. Phys. Lett.* **1994**, *220*, 281.

(15) Brouard, M.; Lambert, H. M.; Rayner, S. P.; Simons, J. P. *Mol. Phys.* **1996**, *89*, 403.

(16) Han, K.-L.; He, G.-Z.; Lou, N.-Q. *J. Chem. Phys.* **1996**, *105*, 8699.

(17) Han, K.-L.; He, G.-Z.; Lou, N.-Q. *J. Chem. Phys.* **1992**, *96*, 7865.

(18) Han, K.-L.; He, G.-Z.; Lou, N.-Q. *Chem. Phys. Lett.* **1992**, *193*, 165.

(19) Han, K.-L.; He, G.-Z.; Lou, N.-Q. *Chem. Phys. Lett.* **1993**, *203*, 509.

(20) Prisant, M. G.; Rettner, C. T.; Zare, R. N. *J. Chem. Phys.* **1981**, *75*, 2222.

(21) Hsu, D. S. Y.; Weinstein, N. D.; Herschbach, D. R. *Mol. Phys.* **1975**, *29*, 257.

(22) Ding, G.; Yang, W.; Sun, W.; He, G.; Lou, N. *Chem. Phys. Lett.* **1994**, *220*, 1.

(23) Yang, W.; Ding, G.; Sun, W.; Xu, D.; He, G.; Lou, N. *Chem. Phys.* **1995**, *193*, 345.

(24) Wang, W. L.; Han, K. L.; He, G. Z. *J. Chem. Phys*. **1998**, *109*, 5446.

(25) Zhan, J. P.; Yang, H. P.; Han, K. L.; Deng, W. Q.; He, G. Z.; Lou, N. Q. *J. Phys. Chem. A* **1997**, *101*, 7486.

(26) Wang, W. L.; Han, K. L.; Zhan, J. P.; Wu, V. W. K.; He, G. Z.; Lou, N. Q. *Chem. Phys. Lett.* **1997**, *278*, 307.

(27) Teule, J. M.; Janssen, M. H. M.; Bulthuis, J.; et al. *J. Chem. Phys*. **1999**, *110*, 10792.

(28) Keizer, F.; Teule, J. M.; Bulthuis, J.; De Graaff, G. J.; Hilgeman, M. H.; Janssen, M. H. M.; Van Kleef, E. H.; Van Leuken, J. J.; Stolte, S. *Chem. Phys*. **1996**, *207*, 261.

(29) Keizer, F.; Bulthuis, J.; Stolte, S. *Isr. J. Chem.* **1994**, *34*, 77.

(30) Johnson, M. A.; Allison, J.; Zare, R. N. *J. Chem. Phys.* **1986**, *85*, 5723.

(31) Cai, M. Q.; Zhang, L.; Tang, B. Y.; Chen, M. D.; Yang, G. W.; Han, K. L. *Chem. Phys.* **2000**, *255*, 283.

(32) Odiorne, T. J.; Brooks, P. R.; Kasper, J. V. V. *J. Chem. Phys.* **1971**, *55*, 1980.

(33) Cox, J. D.; Pilcher, G. *Thermochemistry of Organic and Organometallic Compounds*; Acamic Press: New York, 1970.

(34) Siegel, A.; Schultz, A. *J. Chem. Phys*. **1980**, *72*, 6227.

(35) Han, K. L.; Zheng, X.-G.; Sun, B.-F.; He, G.-Z. *Chem. Phys. Lett.* **1991**, *181*, 474.

(36) Luntz, A. C.; Andresen, P. *J. Chem. Phys.* **1980**, *72*, 5851.